Food & Function

Metabolomics Analysis of Time-Series Human Small Intestine Lumen Samples Collected in vivo

Journal:	*Food & Function*
Manuscript ID	FO-ART-05-2021-001574.R1
Article Type:	Paper
Date Submitted by the Author:	27-Jul-2021
Complete List of Authors:	Folz, Jacob; University of California Davis, Food Science and Technology Shalon, Dari; EnvivoBio Fiehn, Oliver; University of California, Davis, Department of Molecular and Cellular Biology + Genome Center

Metabolomics Analysis of Time-Series Human Small Intestine Lumen Samples Collected *in vivo*

Jacob S. Folz[a], Dari Shalon[b], Oliver Fiehn*[a]

[a] West Coast Metabolomics Center and Department of Food Science and Technology, University of California Davis, Davis, CA, USA

[b] EnVivo Bio, Inc., San Carlos, CA 94070, USA

Abstract

The human small intestine remains an elusive organ to study due to the difficulty of retrieving samples in a non-invasive manner. Stool samples as a surrogate do not reflect events in the upper gut intestinal tract. As proof of concept, this study investigates time-series samples collected from the upper gastrointestinal tract of a single healthy subject. Samples were retrieved using a small diameter tube that collected samples in the stomach and duodenum as the tube progressed to the jejunum, and then remained positioned in the jejunum during the final 8.5 hours of the testing period. Lipidomics and metabolomics liquid chromatography tandem mass spectrometry (LC-MS/MS) assays were employed to annotate 828 unique metabolites using accurate mass with retention time and/or tandem MS library matches. Annotated metabolites were clustered based on correlation to reveal sets of biologically related metabolites. Typical clusters included bile metabolites, food metabolites, protein breakdown products, and endogenous lipids. Acylcarnitines and phospholipids were clustered with known human bile components supporting their presence in human bile, in addition to novel human bile compounds 4-hydroxyhippuric acid, N-acetylglucosaminoasparagine and 3-methoxy-4-hydroxyphenylglycol sulfate. Food metabolites were observed passing through the small intestine after meals. Acetaminophen and its human phase II metabolism products appeared for hours after the initial drug treatment, due to excretion back into the gastrointestinal tract after initial absorption. This exploratory study revealed novel trends in timing and chemical composition of the human jejunum under standard living conditions.

1. Introduction

The human gastrointestinal tract (GI tract) performs essential functions for life including absorption of energy from food and vitamin transformations. This makes the GI tract an important area of research to better understand how humans interact with food. The upper human GI tract has been investigated using techniques such as endoscope imaging[1] and sampling[2], external imaging[3], ileostomy studies[4,5], *in vitro* small intestine models[6], and humanized animal models[7]. These techniques have been primarily used for single timepoint sample collections. However, the human small intestine is a highly complex and dynamic system requiring time-series profiles to understand the *in vivo* functionality of the upper GI tract[8]. This study investigates a unique set of samples collected from the upper GI tract of a single healthy subject at approximately 30-minute intervals for 8 hours.

One important class of biofluids for human GI tract function is bile. Bile is made in the liver, stored in the gallbladder, and excreted into the duodenum. Bile consists of roughly 95% water with 5% organic and inorganic components including bile acids, bile pigments, phospholipids, cholesterol, electrolytes, and proteins[9]. Bile is excreted in response to meals[10] and has important functions including acting as a lipid emulsion stabilizer[11,12] to aid in lipid absorption, as excretory route for cholesterol and other exposome

metabolites[13], and to modify the composition of gut microbiota[14]. To better understand how the GI tract interacts with diet and lifestyle, we investigated bile related metabolites and bile excretion patterns over the course of 8 hours in a single test subject.

In addition to endogenous metabolites, exogenous compounds from food and drugs and their metabolites also pass through the small intestine. These compounds represent extremely broad classes of chemicals encompassing the metabolome of plants, animals, microbes, and the environment. While many exposome compounds are listed in databases such as FooDB and DrugBase, nontargeted metabolomics can detect additional compounds to add knowledge on transformations in the human GI tract. Such food biomarkers may classify dietary patterns and be used in human cohort studies[15–17]. We show here that some foods are more readily predicted from GI tract fluid analyses than others. We also demonstrate the utility of a non-targeted metabolomics analysis leading to novel observations of endogenous and exogenous metabolite dynamics associated with the human GI tract *in vivo*.

2. Methods

Ethics approval

The study was approved by and complied with the guidelines approved by the Association for the Accreditation of Human Research Protection Programs (AAHRPP) certified review board WCG IRB (Study Number 1186513, IRB Tracking Number: 20181298) as a Non-Significant-Risk study not requiring an Investigational Device Exemption (IDE) review by the FDA. The single participant provided written informed consent for study participation conducted at Silicon Valley Gastroenterology, 2490 Hospital Drive, Suite 211, Mountain View, California 94040. For the chemical analyses of samples delivered to UC Davis, the UC Davis IRB Administration approved the study under IRB ID 1307967-1.

Sample Collection

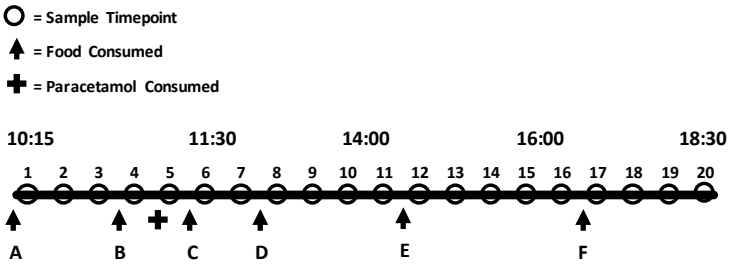

Figure 1. Method summary of GI tract sampling. Timeline of sample collections that occurred at approximately 30-minute intervals throughout one day. *Cross*: 500 mg acetaminophen. *Black arrows*: food or beverage consumption. (A) apple juice, espresso (B) 60 g puree (pear, peach, pumpkin, apple, cinnamon) (C) 10 g puree as before. (D) 20 g olive oil, 20 g white bread, espresso (E) 25 g whole wheat cereal, water, espresso (F) 210 g fermented milk drink. Samples 1-2 were collected from the stomach and 3-20 were collected from the small intestine.

A single human volunteer, a male between the age of 45-65 years without any known morbidities and a BMI <30 swallowed a 1.2 mm outer diameter silicon tube with one end attached to a capsule shaped sinker element 6 mm in diameter and 15 mm long. A silicone tube ran through the center of this sinker element with an opening covered with a 150-micron mesh filter. The capsule was swallowed with water and the tube was stopped from advancing when the end of the tube was 200 cm past the mouth, which equates to 125 cm past the pylorus, placing the sampling end of the tube in the jejunum. Samples were aspirated by pulling out one milliliter aliquots of GI tract fluid using a syringe attached to the proximal end of the sampling tube every 30 minutes. The first two samples were collected while the tube was still in the stomach and the rest were taken from the upper small intestine with the

final 14 samples taken from 125 cm past the pylorus (Supplementary Table 1). During the sample collection period, food, water, and acetaminophen were consumed *ad libitum* and time of ingestion recorded (Figure 1). Specific timepoints of sample collection, food consumption, and sample details can be found in Supplementary Table 1. Samples were transferred to microcentrifuge tubes and frozen at -20 °C until sample extraction (less than 1 week). After sampling, the silicon tube was cut and evacuated along with the capsule sinker element through normal bowel movement.

Sample Preparation

Samples were separated into hydrophobic and hydrophilic portions using a modified liquid bilayer extraction[18]. Frozen samples were thawed on ice and 20 μL of intestinal liquid was transferred to a clean microcentrifuge tube. Blank samples were created using 20 μL of LC-MS grade water instead of intestinal fluid. 225 μL of ice-cold methanol (containing internal standards[19]) was added to each microcentrifuge tube. Tubes were vortexed vigorously for 10 seconds and then 750 μL of methyl-*tert* butyl ether (containing internal standard cholesterol ester 22:1) was added to each tube. All tubes were vortexed vigorously for 10 seconds and shaken on an orbital shaker at 4 °C for 6 minutes. 190 μL of ice-cold water was added to each tube followed by 10 seconds of mixing by vortex. Microcentrifuge tubes were centrifuged at 14,000 RCF for two minutes. Two aliquots of 350 μL of the upper MTBE layer were aliquoted into two clean microcentrifuge tubes for lipidomic analysis, and two aliquots of 125 μL of the lower layer was transferred into two clean microcentrifuge tubes for analysis of hydrophilic metabolites. A portion from the remaining upper and lower layers from all samples were combined with portions of other GI tract samples external to this study to generate pooled quality control samples to assess technical variation in analytical measurement. All tubes were dried to completion in a rotary vacuum dryer and stored at -20 °C for less than two weeks until LC-MS/MS analysis.

LC-MS/MS analysis

Reverse phased liquid chromatography tandem mass spectrometry (RPLC-MS/MS) was used to perform lipidomic analysis and began by adding 100 μL run solvent (9:1 methanol/toluene (*v/v*)) to microcentrifuge tubes from the dried upper layer of extraction. Tubes were vortexed for 10 seconds, sonicated for 2 minutes, vortexed for 10 seconds, centrifuged at 14,000 RCF for 2 minutes and the supernatant was transferred to amber 2 mL LC-MS vials with 200 μL glass insert. Chromatography was performed using a Vanquish Focus UHPLC (ThermoFisher Scientific) and mass spectra collected with a QExactive HF$^+$ mass spectrometer. An Acquity UPLC CSH C18 (100 mm × 2.1 mm, 1.7 μm particle size) column (Waters, Milford MA) with an Acquity UPLC CSH C18 (5 mm × 1.2 mm, 1.7 μm particle size) pre-column (Waters, Milford MA) was used with mobile phase A (6:4 acetonitrile/ water (*v/v*)) and mobile phase B (9:1 isopropanol acetonitrile (*v/v*)). Mobile phases A and B were modified with 10mM ammonium formate and 0.1% formic acid for positive mode ionization, and 10mM ammonium acetate for negative mode ionization. The LC gradient started at 15% B, increased to 30% B from 0-2 minutes, increased to 48% B from 2-2.5 minutes, increased to 82% B from 2.5-11 minutes, increased to 99% B from 11-11.5 minutes, held at 99% B from 11.5-12 minutes, returned to 15% B from 12-12.1 minutes and held at 15% B from 12.1-15 minutes. The autosampler was held at 4 °C and needle wash was performed before and after sample injections for 10 seconds with isopropanol. Injection volumes were 4 μL for both positive and negative mode ionization analyses. Additional MS parameters were used as previously reported[19]. Spectral data was collected with scan range of 120-1700 *m/z*. MS/MS fragmentation used data dependent acquisition (DDA) and was collected for the top 4 most abundant ions from each MS scan.

Hydrophilic interaction liquid chromatography tandem mass spectrometry (HILIC-MS/MS) was used to measure hydrophilic metabolites and began by adding 0.1 mL run solvent (8:2 acetonitrile/water (*v/v*) with 20 deuterated or synthetic internal standards as previously reported[19] to dried microcentrifuge tubes from the bottom aqueous phase of extraction. Tubes were vortexed, sonicated, vortexed, centrifuged, and transferred as in the lipidomic analysis. The same instruments and parameters were used as lipidomic analysis with the following exceptions. A BEH Amide (150 mm × 2.1 mm, 1.7 μm particle size) column (Waters, Milford MA) with BEH Amide (5 mm × 1.2 mm, 1.7 μm particle size) pre-column Waters, Milford MA) was used with mobile phases A (water) and B (95:5 acetonitrile/ water (*v/v*)) both modified with 10mM ammonium formate, and 0.1% formic acid. The gradient started at 100% B, was held at 100% B from 0-2 minutes, decreased to 70% B between 2-7.7 minutes, decreased to 40% between 7.7 and 9.5 minutes, was held at 40% B from 9.5-12.75 minutes, returned to 100% B between 12.75-12.85 minutes, and was held at 100% B from 12.85-17 minutes. Needle wash solution was 1:1 acetonitrile/ water (*v/v*). Injection volumes were 3 μL for positive mode electrospray analyses and 5 μL for negative mode electrospray analyses. The scan range was 90-900 *m/z* with MS/MS acquired using DDA. Four quality control samples were analyzed evenly spaced throughout samples for all analytical platforms and used to assess injection reproducibility and instrument stability.

Data Analysis

LC-MS/MS data was processed using open source software MS-DIAL[20] (version 4.24) which performed peak picking, deisotoping, automated peak annotation, alignment and gap filling. Data processing parameters can be found in Supplementary Table 2. Blank subtraction was performed by removing features that had a maximum sample intensity / average blank intensity ratio of less than 5 and also any features that had a maximum sample intensity of less than 30k. Adduct and duplicate features were flagged using Mass Spectral Feature List Optimizer (MS-FLO)[21]. Data from each of the four analytical platforms (RPLC-MS/MS ESI+/-, HILIC-MS/MS ESI+/-) were processed separately and combined after data curation. No data normalization was performed because no trend in data intensities was observed from the internal standards during data acquisition. Peak height was used for all quantitation. Raw data may be found on the Metabolomics Workbench (ST001794). Metabolite annotations were made using defined confidence levels[22] based on accurate mass, MS/MS library matching to experimental data, and retention time from authentic standards run on the same instrument (Table 1). Tandem MS/MS libraries of the MassBank of North America (MassBank.us) and NIST17 (NIST, Gaithersberg, MD) were used for spectral matching. Manual curation of datasets was performed to reduce in-source fragment annotations identified by very similar RT and high correlation between features. Predicted retention times calculated using Retip[23] were used to help identify in-source fragments and eliminate low confidence annotations. Manual review of MS/MS matches was performed to remove poor spectral

Table 1. Classes of annotated metabolites. Subclass level ontology determined by ClassyFire software. Subclasses < 10 metabolites omitted.

Chemical subclass	count
Amino acids, peptides, and analogues	325
Glycerophosphocholines	57
Carbohydrates and carbohydrate conjugates	45
Fatty acids and conjugates	45
Triacylglycerols	31
Fatty acid esters	23
Glycosphingolipids	20
Phosphosphingolipids	16
Ceramides	13
Diacylglycerols	12
Amines	10
Bile acids, alcohols and derivatives	10

matches since false positive annotations can occur when automatically matching MS/MS from complex biological samples to large MS/MS spectral libraries[24].

Correlation based clustering was performed using the "hclust" function from r package "stats v3.6.2" with method "ward.D2"[25] and tree cutting was conducted using "cutree" function from "stats v3.6.2" with input of k=18-26. Spearman rank correlations were used for all correlation analyses in this study. The optimal number of clusters calculated through the elbow, and silhouette[26] methods using Nbclust R package[27] suggested 2 and 3 as the optimal number of clusters respectively for the 828 annotated metabolites. This few of clusters was not useful to find biologically relevant trends due to large and variable clusters. Using a previous timeseries metabolomics study[28] as a guide, a value of 26 clusters was chosen as a starting point, and then the number of clusters was reduced by 1 until biologically distinct metabolite clusters with differing metabolite profiles began to be combined which resulted in 20 being chosen as the optimal number of clusters (Supplementary Figure 1). Helpful R source scripts for the clustering analysis was adapted from others[29]. Other figures, tables, and correlation analyses were created using custom R scripts.

3. Results and Discussion

Analyses of GI tract metabolites

A total of 828 unique metabolites were annotated using non-targeted UHPLC-MS/MS analyses of samples retrieved from the upper GI tract. The most abundant chemical subclasses encompassed in this dataset are summarized in Table 1. The largest chemical subclass is amino acids, peptides and analogues

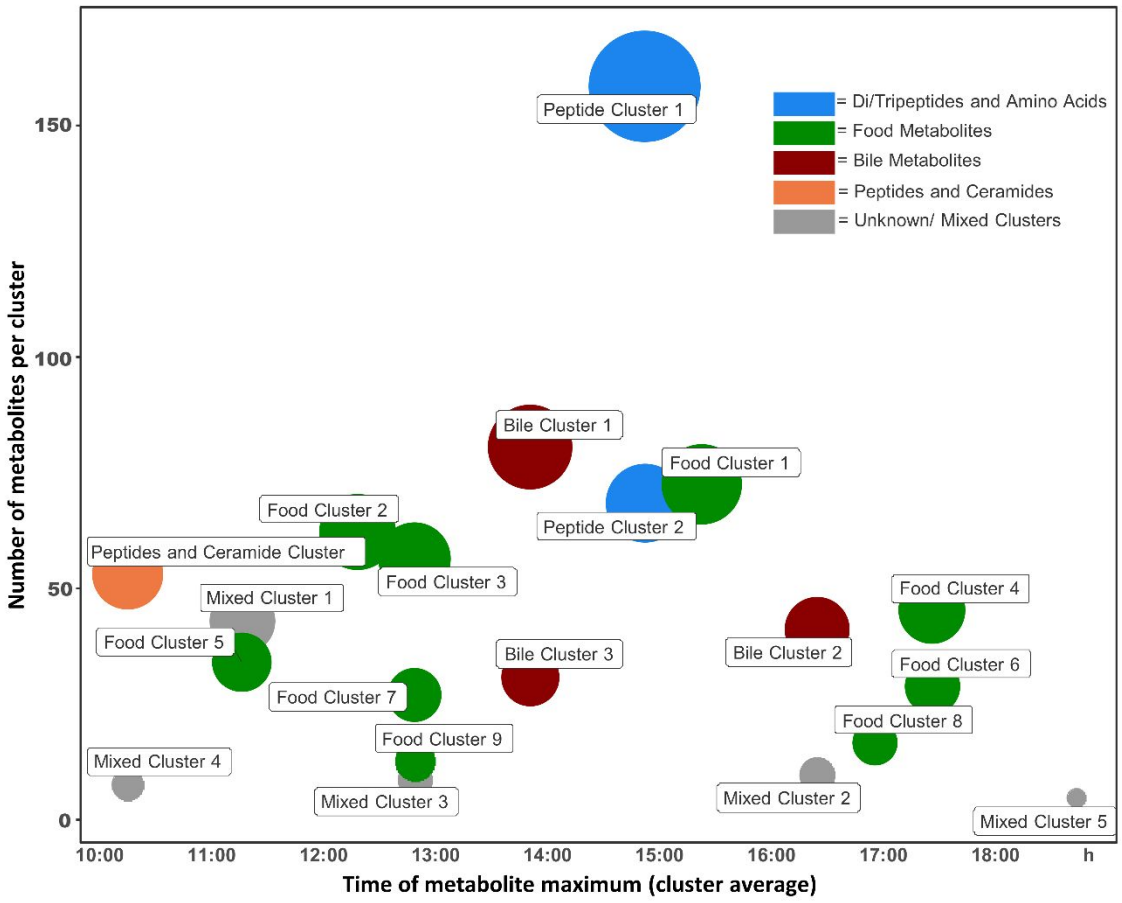

Figure 2. Metabolite groups using correlation-based clustering. The number of metabolites per cluster is represented by node size and position on the y-axis. The position on the x axis gives the time of day at which the clustered metabolites showed an average maximum. Cluster names are given manually by key metabolites in each cluster.

which contains 325 metabolites including 267 dipeptides and tripeptides. The internal standard 12-(cyclohexylcarbamoylamino)dodecanoic acid (CUDA) was used to determine injection reproducibility with raw average relative standard deviations in the quality control between 4-10% for all LC-MS/MS assays (Supplementary Table 4). Metabolites were annotated based on a combination of accurate mass, tandem mass spectral library matching, and retention time matching leading to level 1 through 3 identification confidence levels as previously defined[22]. In total, 6902 chromatographic features with associated MS/MS spectra were detected after blank subtraction, and 12% of these features were annotated with a chemical structure. Unknown features were omitted from the current report, but data are publicly available to enable discovery of additional metabolites in the future (see methods). Metabolites that share biological regulation or origin will strongly correlate in intensity across the testing period. Therefore, we used correlation-based clustering to identify these groups of functionally related metabolites (Figure 2). Multiple clusters were found following consumption of different foods. For example, after consumption of a puree of fruit and vegetables, a group of sugars and arbutin (a biomarker of pear consumption[30–32]) were clustered (Food cluster 5 in Figure 2) and show maximum

intensities approximately 30 minutes after puree consumption (Figure 3A). In total 20 clusters were generated and manually categorized based on the biological function of metabolites within each cluster. Clusters were manually classified as containing a high proportion of food metabolites, bile metabolites, di- and tripeptides and amino acids, and one cluster of di- and tripeptides with many ceramide lipids. Clusters were labeled as mixed/unknown if a cluster contained metabolites split between multiple or unknown functions. The cluster assignment for all metabolites can be found in Supplementary Table 4.

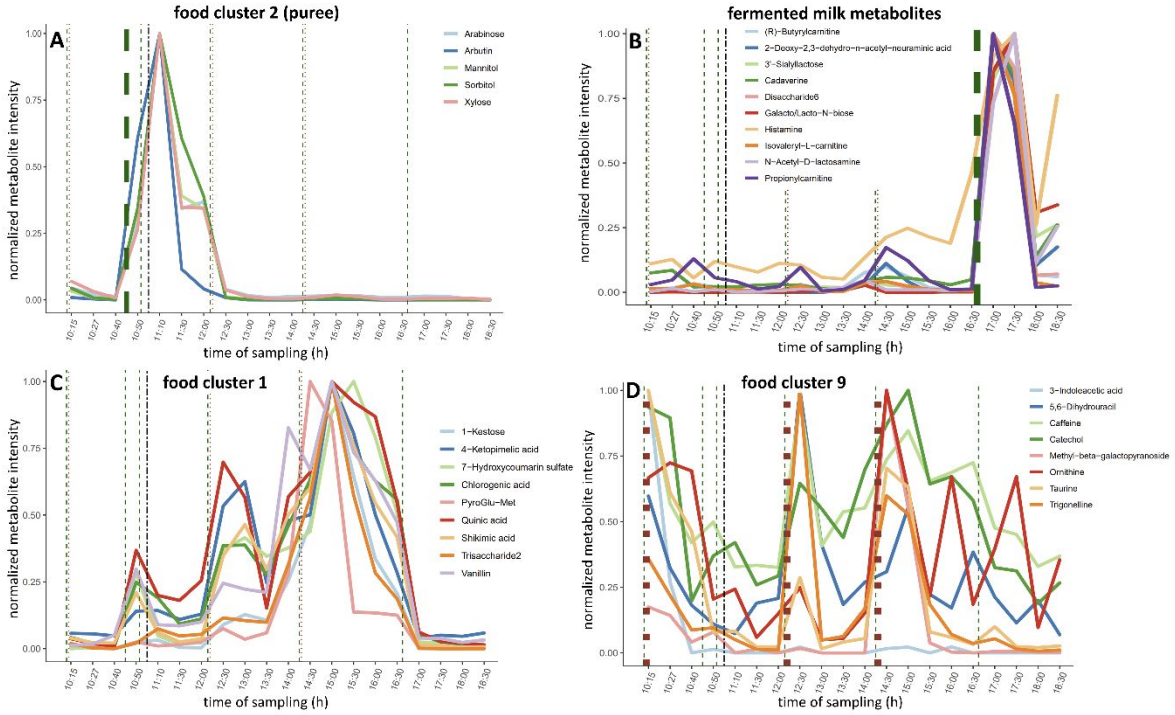

Figure 3. Intensity profiles of food related metabolites across the sampling period. Vertical lines represent meals (green dashed lines), coffee consumption (brown dotted lines) and acetaminophen consumption (black dashed line). Panel A: bold green dashed line for fruit/vegetable puree. Panel B: bold green dashed line for fermented milk beverage. Panel C: metabolites grouped in food cluster 1 without direct relationship to timing of puree consumption. Panel D: bold brown dashed lines for coffee consumption.

3.1 Food related metabolites

Several meals and beverages were consumed during the sample collection period between 10:15 – 18:30 h (Figure 1, Supplementary Table 1). Some meals led to food metabolite clusters unique to a single meal like arbutin and sugars linked to a fruit puree (Figure 3A). These food metabolites showed a clear maximum after food consumption, and then decreased to baseline levels. Similarly, some metabolites were relatively unique to milk (oligosaccharide sialyllactose[33,34], N-acetyl-lactosamine[34], butyrylcarnitine[35]) or fermented milk (cadaverine[36]) and showed distinct maximum levels after consumption of a fermented milk product at 16:35 h (Figure 3B). Alternatively, some food related clusters did not clearly indicate which meal the metabolites came from. One example of a non-specific food metabolite cluster is food cluster 1 which did not contain metabolites unique to a specific meal and had multiple spikes in intensity throughout the day (Figure 3C). Similarly, food cluster 9 also showed multiple spikes throughout the day with high variability. Cluster 9 consisted of coffee biomarkers (trigonelline[37,38],

caffeine[37,38] and catechol[39]) which generally follow coffee consumption timepoints (Figure 3D) linking this cluster to drinking coffee products. These metabolites did not show well-defined peaks after coffee consumption. A previous study reported that coffee metabolites dwell for a long time after coffee consumption by quantifying trigonelline in saliva samples 16 hours after coffee consumption even after rinsing of the mouth[40]. Our study here confirms that some metabolites from food and beverage can remain in the upper GI tract for long periods after consumption. Some metabolites correlated with coffee biomarkers might be caused by an endogenous response to coffee intake, which warrants an interesting aspect for future investigations

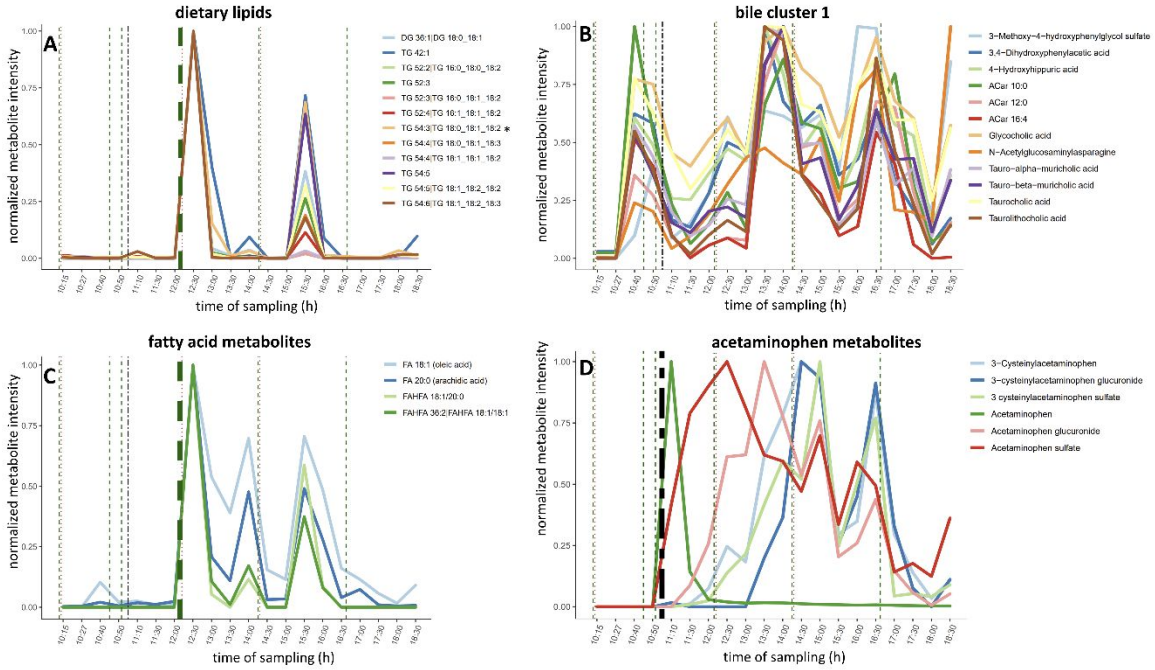

Figure 4. Intensity profiles of metabolite clusters across the sampling period. Vertical lines represent meals (green dashed lines) and acetaminophen consumption (black dashed line). Panel A: bold green dashed line for olive oil / bread with profiles of dietary lipids. Panel B: intensity profiles of 12 bile-associated metabolites. Panel C: bold green dashed line for olive oil / bread with profiles of fatty acids and FAHFAs. Panel D: bold black dashed line for acetaminophen intake, followed by profile of acetaminophen metabolite profiles. *marked annotation encompasses TG 18:0_18:1_18:2, and TG 18:1_18:1_18:1 due to coelution.

Well-defined maxima in intensity of dietary diacylglycerides (DGs) and triacylglycerides (TGs) were observed immediately following consumption of 20 grams of olive oil with a slice of bread at 12:15 h (Figure 4A). TGs are the main component of olive oil. The most common acyl chain lengths in olive oil are 18:1, 18:2, 16:0, and 18:0[41,42]. As expected, these same acyl chain lengths were highly represented in the TGs measured after olive oil consumption (Figure 4A). The profile of free fatty acids showed less defined peaks throughout the sampling period such as oleic acid (fatty acid 18:1) which became more abundant after olive oil consumption but fluctuated in intensity for the rest of the afternoon (Figure 4C). This trend may be explained by TGs of olive oil being hydrolyzed to free fatty acids by lipases present in the upper GI tract, followed by gradual absorption of the fatty acids over the following hours[43,44]. Interestingly, we observed a second spike of the same TGs three hours after olive oil consumption (Figure 4A). One explanation for this second peak is the highly variable gastric retention time of humans which can be between 0 and 4 hours depending on food type[45,46] . This finding implies that some olive oil proceeded

directly to the small intestine after consumption and the rest remained in the stomach with the solid bread of the meal until gastric emptying occurred hours later. The physical appearance of samples supports these findings as there was a lipid layer that formed on the top of the samples with high lipid abundance (samples collected from 12:30-13:00 h and 15:30-16:00 h), and not in samples between the two abundant dietary TG spikes (Supplementary Table 1). Oleic acid (fatty acid 18:1) and arachidic acid (fatty acid 20:0) had higher abundances after olive oil consumption and showed maximum intensities at the same timepoints as the dietary TGs previously mentioned. Two fatty acyl esters of hydroxy fatty acids (FAHFAs) showed similar intensity profiles to oleic and arachidic acid (Figure 4C). FAHFAs are a recently discovered class of lipids that have been shown to decrease insulin resistance and inflammation[47]. FAHFAs are produced endogenously[47] and also found in a variety of plants.[48,49] These FAHFAs are likely derived from olive oil given their strong correlation with other olive oil metabolites and their related fatty acyl constituents (Figure 4C). We here report for the first time the presence of oleic acid-hydroxy oleic acid and oleic acid-hydroxy stearic acid FAHFAs in association with olive oil, and for the first time the finding of FAHFAs in the human GI tract. Finding these FAHFA constituents closely correlated with free fatty acids associated with olive oil suggests that FAHFAs are likely hydrolyzed and absorbed at similar rates compared to free fatty acids.

3.3 Bile related metabolites

Three separate metabolite clusters of bile-related metabolites were found with average maxima at 14:00 h and 16:30 h (Figure 2). These data suggest that over the course of 8 hours of sampling there were two primary bile excretion events, accompanied with lesser bile acid excretion events occurring throughout the sampling period such as a smaller peak at 12:30 h (Figure 4B). These excretion events are characterized by the relative maxima of known bile related metabolites including all twelve detected bile acids, three steroid hormones, cholesterol, phase II exposome metabolites, phospholipids, and acylcarnitines[50,51] (Figure 2, Supplementary Table 4, Supplementary Figure 2B and 2D). Apart from the key bile acids, bile cluster 3 mostly contained phosphatidylcholines (PCs) and cluster 1 had many lysophosphatidylcholines (LPCs), which are both known components of human bile. These clusters have maxima at similar timepoints compared to bile acids but show more defined spikes and then drop to baseline levels for the remainder of the samples, likely due to rapid lipase action on PCs and LPCs (Supplementary Figure 2). Bile acids are the most focused on of bile components due to their importance in food digestion[12], cell injury and protection[52], and function as a signaling axis between the gut microbiota and host[53].

Bile acids are difficult to study in humans *in vivo* due to difficulty in sampling the human small intestine making this a valuable and unique view into bile excretion under normal conditions. The time dependent excretion of bile appeared to be strongly related to passage of dietary lipids through the upper small intestine. Lipids linked to dietary sources showed two sharp spikes in abundance at 12:30 h and 15:30 h (Figure 4A). One hour after these spikes in lipid concentrations, major bile excretion events were recorded at 13:30 h and 16:30 h (Figure 4B). This observation is in alignment with the known progression of lipid rich stomach chyme stimulating cells of the proximal small intestine to release hormone cholecystokinin into circulation leading to contraction of the gallbladder and excretion of bile into the intestinal tract[54]. The postprandial response of bile components also aligns with the finding that bile acids in circulation are governed by meal intake, as opposed to hepatic bile acid synthesis, which has a defined circadian rhythm[55]. Previous studies of bile excretion report “time after test meal” to predict gallbladder contraction[3,10,56,57]. In our study, we are better able to give a specific metric of dietary lipids in the small

intestine to better measure the excretion of bile compared to time after consuming meals. Our study gives a unique perspective on the time dependency of known bile metabolite excretion relating to dietary lipids.

In addition, we found a range of both known and novel metabolites to be correlated with bile. Specifically, the metabolite 4-hydroxyhippuric acid is clustered with bile metabolites and has a Spearman rank correlation coefficient of $r_{xy} > 0.9$ to six different bile acids and several other bile related metabolites (Supplementary Table 5). This metabolite is a product of microbial transformation of dietary polyphenols followed by liver transformation and glycination[58] and has been reported as a urinary biomarker for fruit and vegetable intake in humans[59]. Metabolite 4-hydroxyhippuric acid has been measured in mouse bile[60], however this is the first report of this metabolite detected in relation to human bile. Another metabolite, N-acetylglucosaminylasparagine, is a glycoprotein breakdown product reported to be disposed of through urine[61] and is here associated with bile metabolites suggesting bile as an additional disposal route for this metabolite. Another metabolite clustered with bile metabolites is a product of norepinephrine metabolism, 3-methoxy-4-hydroxyphenylglycol sulfate. This metabolite has been reported as a urinary metabolite, but not as a bile related metabolite. It has been previously proposed that bile is a plausible disposal route for 3-methoxy-4-hydroxyphenylglycol sulfate in addition to urine[62]; however, we here present the first direct measurements to validate this link. Urine and bile are routes of excretion for metabolic end products and exogenous metabolites[13] which makes the link of these known urinary metabolites in bile for the first time a plausible biological outcome.

3.4 Acetaminophen and related metabolites

A dose of 500 mg of the general analgesic acetaminophen was taken orally mid-morning on the day of this experiment (Figure 1). Acetaminophen abundance in the upper GI tract lumen immediately rose to its highest level 15 minutes later. After 35 minutes the abundance of acetaminophen fell to about 15% of its maximal abundance and continued to fall to baseline level over the following hours. After absorption, acetaminophen is transformed in the liver primarily to acetaminophen sulfate, acetaminophen glucuronide, and cysteinylacetaminophen[63,64]. These three conjugates were detected, and the intensity profiles support the route of liver transformation of acetaminophen, biliary excretion, and collection from the upper small intestine (Figure 4D). Interestingly, each conjugate showed a unique profile. Acetaminophen sulfate appeared immediately after acetaminophen ingestion and had a maximal abundance after 1.5 hours, in contrast to acetaminophen glucuronide that did not appear until 30 minutes after acetaminophen ingestion and had maximal abundance after 2.5 hours. The phase III conjugate 3-cysteinylacetaminophen slowly increased in abundance and did not reach maximal intensity until 3.5 hours after acetaminophen ingestion (Figure 4D). Biliary excretion of these conjugated metabolites is further supported as the source of these metabolites because we detected a local maximum for these conjugates at 16:30 h, the same timepoint as found for one of the major bile excretion events (Figure 4B). The unique profile for each of these acetaminophen related metabolites is in agreement with the known pharmacokinetic properties of acetaminophen. After oral ingestion of acetaminophen, plasma acetaminophen has maximum concentration within less than 1 hour, followed by the maximum of the sulfate conjugate between 1 and 1.5 hours, and the glucuronide conjugate maximum at 2 to 2.5 hours[64]. The immediate appearance of acetaminophen sulfate in this experiment, and no immediate appearance in acetaminophen glucuronide, is expected because intestinal epithelium cells have the capacity to convert acetaminophen to acetaminophen sulfate *in vitro*, while showing little to no capacity to convert acetaminophen to acetaminophen glucuronide[65].

Next, we wondered if additional downstream metabolites of acetaminophen might be detectable in the GI tract. To make this end, we used the BioTransformer software[66] that predicts possible metabolic products of drugs using known phase II metabolism reactions from humans. BioTransformer predicted the presence of acetaminophen sulfate and acetaminophen glucuronide from acetaminophen, however 3-cysteinylacetaminophen was not predicted, likely because it requires multiple reactions to form (conjugation to glutathione then degradation to 3-cysteinylacetaminophen[67]). Importantly, BioTransformer predicted additional acetaminophen metabolites for which no public MS/MS spectra are available, neither in MassBank.us nor NIST20. Instead, we queried unknown LC-MS/MS features using accurate mass matches to the candidate list provided through BioTransformer. Two BioTransformer candidate accurate mass matches were 3-cysteinylacetaminophen glucuronide and 3-cysteinylcysteine acetaminophen sulfate, both with less than 1.8 ppm mass difference to the theoretical elemental compositions. The glucuronide conjugate was too low abundant to trigger a data-dependent MS/MS event, but the MS/MS spectrum for the 3-cysteinylcysteine acetaminophen sulfate included a typical M-80 representing neutral loss of SO_3, confirming the likely identification of this compound (Supplementary Table 4). While these two metabolites have been reported before in urine[68], and other authors predicted these acetaminophen metabolites to occur in mammals[69], no MS/MS spectra were published to date. Both metabolites showed similar time profile as 3-cysteinylacetaminophen (Figure 4D), providing additional biological support for structural annotation of these acetaminophen metabolites. Measurement of these acetaminophen metabolites in relation to bile highlights the use of bile clusters in the GI tract for understanding drug metabolism in humans.

3.5 Ceramide and Peptide Clusters

One cluster of metabolites contained many ceramides with high degree of intercorrelations (Supplementary Figure 2A). Ceramide abundance showed five very pronounced maxima throughout the eight-hour sampling period that did not correlate to other physiological or environmental stimuli such as acetaminophen, dietary ingestions, bile excretions or dietary lipids. Ceramides are important as structural lipids and signaling molecules particularly within the GI tract[70]. These lipids are produced in many tissues throughout the body including GI tract epithelium and are also present in many foods[70]. Our findings presented here support the notion that GI tract ceramides are produced endogenously and are regulated tightly in frequent intervals.

The cluster of GI tract ceramides had maxima that trended with dozens of di- and tripeptides and free amino acids maxima (Supplementary Figure 2C). Such short-chain peptides in these clusters might originate from incomplete protein degradation and found in the GI tract either through gastric or pancreatic excretions. Both the stomach and pancreas secrete proteases that could be responsible for digesting proteins down to short peptides and amino acids. The abundance profile of these clusters show 2-hourly maxima at 10:30h, 12:30h, 14:30h and 16:30h with an additional minor maximum at 13:30h. Similar to ceramides, these maxima did not directly coincide with major bile excretions or dietary lipids. Pancreatic juice is a relatively little investigated biofluid[71]. However, multiple studies have reported a selection of free amino acids as important components of pancreatic juice[71] including phenylalanine, tyrosine, tryptophan, valine, leucine, isoleucine and alanine. We here find all of these amino acids associated with pancreatic juice in conjunction with di- and tripeptide clusters (Supplementary Figure 2B). Di- and tripeptides are regularly reported in metabolomics studies[72,73] but are absent from most classic nutritional studies. Our data support the notion that the observed dipeptide clusters may be derived from

pancreatic juice; yet this evidence is not conclusive because amino acids are certainly not unique to pancreatic juice.

4.0 Conclusions

We here present a technique to enable a unique perspective into the human upper GI tract *in vivo* over the course of eight hours. Correlation based clustering connected metabolites of similar biological function to be investigated in temporal profiles and to be associated with important physiological and dietary events. Interestingly, even classic nutritional compounds like amino acids showed clear temporal profiles that were not exclusively related to dietary input. Bile metabolites spiked roughly 1.5 hours after measurement of dietary lipids passing the upper small intestine. This observation presents a unique measurement because in humans, bile excretion has been measured almost exclusively under fasted conditions and not during a normal day of *ad libitum* meal consumption. We here report specific metabolites (4-hydroxyhippuric acid, N-acetylglucosaminylasparagine, 3-methoxy-4-hydroxyphenylglycol sulfate) to be linked to human bile. This experiment also gave a unique insight into acetaminophen metabolism and excretion and presents the utility of bile associated metabolites to find endogenously modified drug metabolites. The human GI tract is an extraordinarily complex and dynamic system and metabolomics experiments offer a valuable approach to discover how the gut interacts with food. This single subject study presents trends that may not be representative of the general population. Future experiments are needed to determine which trends can be expected from the population as a whole. Although this is a single subject study the dataset is rich in information and provides unique findings into the metabolome of the upper human GI tract *in vivo*.

Conflicts of interest

Dari Shalon is an employee and has an equity interest in Envivo Bio, a company with interest in the human gastrointestinal tract.

Acknowledgements

This study was partly funded through NSF MCB 1611846 and NIH U2C ES030158.

References

1 R. Kiesslich, M. Goetz, E. M. Angus, Q. Hu, Y. Guan, C. Potten, T. Allen, M. F. Neurath, N. F. Shroyer, M. H. Montrose and A. J. M. Watson, Identification of Epithelial Gaps in Human Small and Large Intestine by Confocal Endomicroscopy, *Gastroenterology*, 2007, **133**, 1769–1778.

2 C. L. Wright and R. H. Riddell, Histology of the Stomach and Duodenum in Crohn's Disease, *Am. J. Surg. Pathol.*, 1998, **22**, 383–390.

3 P. Portincasa, A. Moschetta, A. Colecchia, D. Festi and G. Palasciano, Measurements of gallbladder motor function by ultrasonography: Towards standardization, *Dig. Liver Dis.*, 2003, **35**, 56–61.

4 L. Ellegård and H. Andersson, Oat bran rapidly increases bile acid excretion and bile acid synthesis: An ileostomy study, *Eur. J. Clin. Nutr.*, 2007, **61**, 938–945.

5 L. Ohlsson, E. Hertervig, B. A. G. Jönsson, R. D. Duan, L. Nyberg, R. Svernlöv and Å. Nilsson, Sphingolipids in human ileostomy content after meals containing milk sphingomyelin, *Am. J. Clin. Nutr.*, 2010, **91**, 672–678.

6 I. Mainville, Y. Arcand and E. R. Farnworth, A dynamic model that simulates the human upper gastrointestinal tract for the study of probiotics, *Int. J. Food Microbiol.*, 2005, **99**, 287–296.

7 Q. Zhang, G. Widmer and S. Tzipori, A pig model of the human gastrointestinal tract, *Gut Microbes*, 2013, **4**, 193–200.

8 E. G. Zoetendal, J. Raes, B. Van Den Bogert, M. Arumugam, C. C. Booijink, F. J. Troost, P. Bork, M. Wels, W. M. De Vos and M. Kleerebezem, The human small intestinal microbiota is driven by rapid uptake and conversion of simple carbohydrates, *ISME J.*, 2012, **6**, 1415–1426.

9 J. L. Boyer, Bile formation and secretion, *Compr. Physiol.*, 2013, **3**, 1035–1078.

10 P. J. Howard, G. M. Murphy and R. H. Dowling, Gall bladder emptying patterns in response to a normal meal in healthy subjects and patients with gall stones: Ultrasound study, *Gut*, 1991, **32**, 1406–1411.

11 A. J. Fillery-Travis, L. H. Foster and M. M. Robins, Stability of emulsions stabilised by two physiological surfactants: l-α-phosphatidylcholine and sodium taurocholate, *Biophys. Chem.*, 1995, **54**, 253–260.

12 M. Armand, P. Borel, B. Pasquier, C. Dubois, M. Senft, M. Andre, J. Peyrot, J. Salducci and D. Lairon, Physicochemical characteristics of emulsions during fat digestion in human stomach and duodenum, *Am. J. Physiol. - Gastrointest. Liver Physiol.*, 1996, **271**, G172-183.

13 M. J. Zamek-Gliszczynski, K. A. Hoffmaster, K. I. Nezasa, M. N. Tallman and K. L. R. Brouwer, Integration of hepatic drug transporters and phase II metabolizing enzymes: Mechanisms of hepatic excretion of sulfate, glucuronide, and glutathione metabolites, *Eur. J. Pharm. Sci.*, 2006, **27**, 447–486.

14 V. Urdaneta and J. Casadesús, Interactions between bacteria and bile salts in the gastrointestinal and hepatobiliary tracts, *Front. Med.*, 2017, **4**, 1–13.

15 J. W. Lampe, Biomarkers of nutritional exposure and nutritional status: An overview, *J. Nutr.*, 2003, **133**, 956–964.

16 M. Garcia-Aloy, M. Ulaszewska, P. Franceschi, S. Estruel-Amades, C. H. Weinert, A. Tor-Roca, M. Urpi-Sarda, F. Mattivi and C. Andres-Lacueva, Discovery of Intake Biomarkers of Lentils, Chickpeas, and White Beans by Untargeted LC–MS Metabolomics in Serum and Urine, *Mol. Nutr. Food Res.*, 2020, **64**, 1901137.

17 F. Madrid-Gambin, C. Brunius, M. Garcia-Aloy, S. Estruel-Amades, R. Landberg and C. Andres-Lacueva, Untargeted 1H NMR-Based Metabolomics Analysis of Urine and Serum Profiles after Consumption of Lentils, Chickpeas, and Beans: An Extended Meal Study to Discover Dietary Biomarkers of Pulses, *J. Agric. Food Chem.*, 2018, **66**, 6997–7005.

18 V. Matyash, G. Liebisch, T. V. Kurzchalia, A. Shevchenko and D. Schwudke, Lipid extraction by methyl- *tert* -butyl ether for high-throughput lipidomics, *J. Lipid Res.*, 2008, **49**, 1137–1146.

19 D. K. Barupal, Y. Zhang, T. Shen, S. Fan, B. S. Roberts, P. Fitzgerald, B. Wancewicz, L. Valdiviez, G. Wohlgemuth, G. Byram, Y. Y. Choy, B. Haffner, M. R. Showalter, A. Vaniya, C. S. Bloszies, J. S. Folz, T. Kind, A. M. Flenniken, C. McKerlie, L. M. J. Nutter, K. C. Lloyd and O. Fiehn, A comprehensive plasma metabolomics dataset for a cohort of mouse knockouts within the international mouse phenotyping consortium, *Metabolites*, 2019, **9**, 9050101.

20 H. Tsugawa, K. Ikeda, M. Takahashi, A. Satoh, Y. Mori, H. Uchino, N. Okahashi, Y. Yamada, I. Tada, P. Bonini, Y. Higashi, Y. Okazaki, Z. Zhou, Z. J. Zhu, J. Koelmel, T. Cajka, O. Fiehn, K. Saito, M. Arita and M. Arita, A lipidome atlas in MS-DIAL 4, *Nat. Biotechnol.*, 2020, **38**, 1159–1163.

21 B. C. DeFelice, S. S. Mehta, S. Samra, T. Čajka, B. Wancewicz, J. F. Fahrmann and O. Fiehn, Mass Spectral Feature List Optimizer (MS-FLO): A Tool To Minimize False Positive Peak Reports in Untargeted Liquid Chromatography-Mass Spectroscopy (LC-MS) Data Processing, *Anal. Chem.*, 2017, **89**, 3250–3255.

22 E. L. Schymanski, J. Jeon, R. Gulde, K. Fenner, M. Ru, H. P. Singer and J. Hollender, Identifying Small Molecules via High Resolution Mass Spectrometry: Communicating Confidence, *Environ. Sci. Technol.*, 2014, **48**, 2097–2098.

23 P. Bonini, T. Kind, H. Tsugawa, D. K. Barupal and O. Fiehn, Retip: Retention Time Prediction for Compound Annotation in Untargeted Metabolomics, *Anal. Chem.*, 2020, **92**, 7515–7522.

24 J. E. Schollée, E. L. Schymanski, M. A. Stravs, R. Gulde, N. S. Thomaidis and J. Hollender, Similarity of High-Resolution Tandem Mass Spectrometry Spectra of Structurally Related Micropollutants and Transformation Products, *J. Am. Soc. Mass Spectrom.*, 2017, **28**, 2692–2704.

25 J. H. Ward, Hierarchical Grouping to Optimize an Objective Function, *J. Am. Stat. Assoc.*, 1963, **58**, 236–244.

26 P. J. Rousseeuw, Silhouettes: A graphical aid to the interpretation and validation of cluster analysis, *J. Comput. Appl. Math.*, 1987, **20**, 53–65.

27 M. Charrad, N. Ghazzali, V. Boiteau and A. Niknafs, Nbclust: An R package for determining the relevant number of clusters in a data set, *J. Stat. Softw.*, 2014, **61**, 1–36.

28 M. J. Rusilowicz, M. Dickinson, A. J. Charlton, S. O'Keefe and J. Wilson, MetaboClust: Using interactive time-series cluster analysis to relate metabolomic data with perturbed pathways, *PLoS One*, 2018, **13**, e0205968.

29 D. K. Barupal and O. Fiehn, Chemical Similarity Enrichment Analysis (ChemRICH) as alternative to biochemical pathway mapping for metabolomic datasets, *Sci. Rep.*, 2017, **7**, 14567.

30 D. C. Nieman, N. D. Gillitt, W. Sha, M. P. Meaney, C. John, K. L. Pappan and J. M. Kinchen, Metabolomics-Based Analysis of Banana and Pear Ingestion on Exercise Performance and Recovery, *J. Proteome Res.*, 2015, **14**, 5367–5377.

31 M. Ulaszewska, N. Vázquez-Manjarrez, M. Garcia-Aloy, R. Llorach, F. Mattivi, L. O. Dragsted, G. Praticò and C. Manach, Food intake biomarkers for apple, pear, and stone fruit Lars Dragsted, *Genes Nutr.*, 2018, **13**, 1–16.

32 A. Escarpa and M. C. González, Evaluation of high-performance liquid chromatography for determination of phenolic compounds in pear horticultural cultivars, *Chromatographia*, 2000, **51**, 37–43.

33 V. Kelly, S. Davis, S. Berry, J. Melis, R. Spelman, R. Snell, K. Lehnert and D. Palmer, Rapid , quantitative analysis of 3 c - and 6 c -sialyllactose in milk by flow-injection analysis – mass spectrometry : Screening of milks for naturally elevated sialyllactose concentration, *J. Dairy Sci.*, 2013, **96**, 7684–7691.

34 K. A. Al Busadah, S. D. Carrington, S. Albrecht, J. A. Lane, K. Marin, R. M. Hickey and P. M. Rudd, A comparative study of free oligosaccharides in the milk of domestic animals, *Br. J. Nutr.*, 2014, **111**, 1313–1328.

35 K. J. Boudonck, M. W. Mitchell, J. Wulff and J. A. Ryals, Characterization of the biochemical variability of bovine milk using metabolomics, *Metabolomics*, 2009, **5**, 375–386.

36 O. Ozdestan and A. Uren, Biogenic amine content of kefir : a fermented dairy product, *Eur. Food Res. Technol.*, 2010, **231**, 101–107.

37 K. A. Guertin, E. Loftfield, S. M. Boca, J. N. Sampson, S. C. Moore, Q. Xiao, W. Y. Huang, X. Xiong, N. D. Freedman, A. J. Cross and R. Sinha, Serum biomarkers of habitual coffee consumption may provide insight into the mechanism underlying the association between coffee consumption and colorectal cancer, *Am. J. Clin. Nutr.*, 2015, **101**, 1000–1011.

38 J. A. Rothwell, P. Keski-Rahkonen, N. Robinot, N. Assi, C. Casagrande, M. Jenab, P. Ferrari, M. C. Boutron-Ruault, Y. Mahamat-Saleh, F. R. Mancini, H. Boeing, V. Katzke, T. Kühn, K. Niforou, A. Trichopoulou, E. Valanou, V. Krogh, A. Mattiello, D. Palli, C. Sacerdote, R. Tumino and A. Scalbert, A Metabolomic Study of Biomarkers of Habitual Coffee Intake in Four European Countries, *Mol. Nutr. Food Res.*, 2019, **63**, 1900659.

39 R. Lang, C. Mueller and T. Hofmann, Development of a stable isotope dilution analysis with liquid chromatography-tandem mass spectrometry detection for the quantitative analysis of di- and trihydroxybenzenes in foods and model systems, *J. Agric. Food Chem.*, 2006, **54**, 5755–5762.

40 R. Lang, A. Wahl, T. Stark and T. Hofmann, in *ACS Symposium Series*, 2012, vol. 1098, pp. 13–25.

41 A. Ranalli, L. Pollastri, S. Contento, G. Di Loreto, E. Iannucci, L. Lucera and F. Russi, Acylglycerol and fatty acid components of pulp, seed, and whole olive fruit oils. Their use to characterize fruit variety by chemometrics, *J. Agric. Food Chem.*, 2002, **50**, 3775–3779.

42 E. Alves, T. Melo, M. P. Barros, M. M. R. Domingues and P. Domingues, Lipidomic Profiling of the Olive (Olea europaea L.) Fruit towards Its Valorisation as a Functional Food: In-depth identification of triacylglycerols and polar lipids in Portuguese olives, *Molecules*, 2019, **24**, 24142555.

43 M. Armand, Lipases and lipolysis in the human digestive tract: Where do we stand?, *Curr. Opin. Clin. Nutr. Metab. Care*, 2007, **10**, 156–164.

44 Z. Ye, C. Cao, R. Li, P. Cao, Q. Li and Y. Liu, Lipid composition modulates the intestine digestion rate and serum lipid status of different edible oils: A combination of in vitro and in vivo studies, *Food Funct.*, 2019, **10**, 1490–1503.

45 R. K. Goyal, Y. Guo and H. Mashimo, Advances in the physiology of gastric emptying, *Neurogastroenterol. Motil.*, 2019, **31**, e13546.

46 S. Hellmig, F. Von Schöning, C. Gadow, S. Katsoulis, J. Hedderich, U. R. Fölsch and E. Stüber, Gastric emptying time of fluids and solids in healthy subjects determined by 13C breath tests: Influence of age, sex and body mass index, *J. Gastroenterol. Hepatol.*, 2006, **21**, 1832–1838.

47 M. M. Yore, I. Syed, P. M. Moraes-Vieira, T. Zhang, M. A. Herman, E. A. Homan, R. T. Patel, J. Lee, S. Chen, O. D. Peroni, A. S. Dhaneshwar, A. Hammarstedt, U. Smith, T. E. McGraw, A. Saghatelian and B. B. Kahn, Discovery of a class of endogenous mammalian lipids with anti-diabetic and anti-

inflammatory effects, *Cell*, 2014, **159**, 318–332.

48 M. J. Kolar, S. Konduri, T. Chang, H. Wang, C. McNerlin, L. Ohlsson, M. Härröd, D. Siegel and A. Saghatelian, Linoleic acid esters of hydroxy linoleic acids are anti-inflammatory lipids found in plants and mammals, *J. Biol. Chem.*, 2019, **294**, 10698–10707.

49 A. M. Liberati-Čizmek, M. Biluš, A. L. Brkić, I. C. Barić, M. Bakula, A. Hozić and M. Cindrić, Analysis of Fatty Acid Esters of Hydroxyl Fatty Acid in Selected Plant Food, *Plant Foods Hum. Nutr.*, 2019, **74**, 235–240.

50 I. M. A. Brüggenwirth, R. J. Porte and P. N. Martins, Bile Composition as a Diagnostic and Prognostic Tool in Liver Transplantation, *Liver Transplant.*, 2020, **26**, 1177–1187.

51 B. L. Shneider, P. Rinaldo, S. Emre, J. Bucuvalas, R. Squires, M. Narkewicz, G. Gondolesi, M. Magid, R. Morotti and L. S. Hynan, Abnormal concentrations of esterified carnitine in bile: A feature of pediatric acute liver failure with poor prognosis, *Hepatology*, 2005, **41**, 717–721.

52 M. J. Perez and O. Britz, Bile-acid-induced cell injury and protection, *World J. Gastroenterol.*, 2009, **15**, 1677–1689.

53 P. B. Hylemon, W. M. Pandak, G. Gil, H. Zhou, S. Ren and P. Dent, Bile acids as regulatory molecules, *J. Lipid Res.*, 2009, **50**, 1509–1520.

54 J. R. Grider, Role of Cholecystokinin in the Regulation of Gastrointestinal Motility, *J. Nutr.*, 1994, **124**, 1334S–1339S.

55 C. Gälman, B. Angelin and M. Rudling, Bile acid synthesis in humans has a rapid diurnal variation that is asynchronous with cholesterol synthesis, *Gastroenterology*, 2005, **129**, 1445–1453.

56 R. P. Jazrawi, P. Pazzi, M. Letizia Petroni, N. Prandini, C. Paul, J. A. Adam, S. Gullini and T. C. Northfield, Postprandial gallbladder motor function: Refilling and turnover of bile in health and in cholelithiasis, *Gastroenterology*, 1995, **109**, 582–591.

57 M. Acalovschi, D. L. Dumitraçcu and I. Csakany, Gastric and gall bladder emptying of a mixed meal are not coordinated in liver cirrhosis - A simultaneous sonographic study, *Gut*, 1997, **40**, 412–417.

58 A. R. Rechner, M. A. Smith, G. Kuhnle, G. R. Gibson, E. S. Debnam, S. K. S. Srai, K. P. Moore and C. A. Rice-Evans, Colonic metabolism of dietary polyphenols: Influence of structure on microbial fermentation products, *Free Radic. Biol. Med.*, 2004, **36**, 212–225.

59 M. Beckmann, T. Wilson, H. Zubair, A. J. Lloyd, L. Lyons, H. Phillips, K. Tailliart, N. Gregory, R. Thatcher, I. Garcia-Perez, G. Frost, J. M. Mathers and J. Draper, A Standardized Strategy for Simultaneous Quantification of Urine Metabolites to Validate Development of a Biomarker Panel Allowing Comprehensive Assessment of Dietary Exposure, *Mol. Nutr. Food Res.*, 2020, **64**, 1–15.

60 N. Orrego-Lagarón, M. Martínez-Huélamo, A. Vallverdú-Queralt, R. M. Lamuela-Raventos and E. Escribano-Ferrer, High gastrointestinal permeability and local metabolism of naringenin: Influence of antibiotic treatment on absorption and metabolism, *Br. J. Nutr.*, 2015, **114**, 169–180.

61 P. Aula, K. O. Raivio and P. Maury, Variation of urinary excretion of aspartylglucosamine and associated clinical findings in aspartylglucosaminuria, *J. Inherit. Metab. Dis.*, 1980, **3**, 159–163.

62 G. Eisenhofer, A. Åneman, D. Hooper, B. Rundqvist and P. Friberg, Mesenteric organ production, hepatic metabolism, and renal elimination of norepinephrine and its metabolites in humans, *J.*

Neurochem., 1996, **66**, 1565–1573.

63 A. Toda, M. Shimizu, S. Uehara, T. Sasaki, T. Miura, M. Mogi, M. Utoh, H. Suemizu and H. Yamazaki, Plasma and hepatic concentrations of acetaminophen and its primary conjugates after oral administrations determined in experimental animals and humans and extrapolated by pharmacokinetic modeling, *Xenobiotica*, 2021, **51**, 316–323.

64 L. Prescott, Kinetics and metabolism of paracetamol and phenacetin., *Br. J. Clin. Pharmacol.*, 1980, **10**, 291S-298S.

65 S. Siissalo, L. Laine, A. Tolonen, A. M. Kaukonen, M. Finel and J. Hirvonen, Caco-2 cell monolayers as a tool to study simultaneous phase II metabolism and metabolite efflux of indomethacin, paracetamol and 1-naphthol, *Int. J. Pharm.*, 2010, **383**, 24–29.

66 Y. Djoumbou-Feunang, J. Fiamoncini, A. Gil-de-la-Fuente, R. Greiner, C. Manach and D. S. Wishart, BioTransformer: A comprehensive computational tool for small molecule metabolism prediction and metabolite identification, *J. Cheminform.*, 2019, **11**, 1–25.

67 M. R. McGill and H. Jaeschke, Metabolism and disposition of acetaminophen: Recent advances in relation to hepatotoxicity and diagnosis, *Pharm. Res.*, 2013, **30**, 2174–2187.

68 E. Pujos-Guillot, G. Pickering, B. Lyan, G. Ducheix, M. Brandolini-Bunlon, F. Glomot, D. Dardevet, C. Dubray and I. Papet, Therapeutic paracetamol treatment in older persons induces dietary and metabolic modifications related to sulfur amino acids, *Age (Omaha).*, 2012, **34**, 181–193.

69 S. J. Hart, I. C. Calder and J. D. Tange, The Metabolism and Toxicity of Paracetamol in Sprague-Dawley and Wistar Rats, *Eur. J. Drug Metab. Pharmacokinet.*, 1982, **7**, 203–222.

70 K. Kurek, B. Łukaszuk, D. M. Piotrowska, P. Wiesiołek, A. M. Chabowska and M. Zendzian-Piotrowska, Metabolism, physiological role, and clinical implications of sphingolipids in gastrointestinal tract, *Biomed Res. Int.*, 2013, **2013**, 908907.

71 N. Cortese, G. Capretti, M. Barbagallo, A. Rigamonti, P. G. Takis, G. F. Castino, D. Vignali, G. Maggi, F. Gavazzi, C. Ridolfi, G. Nappo, G. Donisi, M. Erreni, R. Avigni, D. Rahal, P. Spaggiari, M. Roncalli, P. Cappello, F. Novelli, P. Monti, A. Zerbi, P. Allavena, A. Mantovani and F. Marchesi, Metabolome of pancreatic juice delineates distinct clinical profiles of pancreatic cancer and reveals a link between glucose metabolism and PD-1+Cells, *Cancer Immunol. Res.*, 2020, **8**, 493–505.

72 S. Ichikawa, M. Morifuji, H. Ohara, H. Matsumoto, Y. Takeuchi and K. Sato, Hydroxyproline-containing dipeptides and tripeptides quantified at high concentration in human blood after oral administration of gelatin hydrolysate, *Int. J. Food Sci. Nutr.*, 2010, **61**, 52–60.

73 C. Ibáñez, C. Simó, V. García-Cañas, Á. Gómez-Martínez, J. A. Ferragut and A. Cifuentes, CE/LC-MS multiplatform for broad metabolomic analysis of dietary polyphenols effect on colon cancer cells proliferation, *Electrophoresis*, 2012, **33**, 2328–2336.